Radiation Physics and Chemistry 120 (2016) 1–6

Contents lists available at ScienceDirect

Radiation Physics and Chemistry

journal homepage: www.elsevier.com/locate/radphyschem

The behaviors of anatase and TiO_2(B) phase coexisting nanosheets under high pressure

Yanwei Huang [a,b,*], Wentao Li [a,c], Xiangting Ren [a], Zhenhai Yu [a], Sudeshna Samanta [a], Shuai Yan [d], Jun Zhang [b], Lin Wang [a,*]

[a] Center for High Pressure Science and Technology Advanced Research, Shanghai 201203, China
[b] College of Materials and Environmental Engineering, Hangzhou Dianzi University, Hangzhou 310018, China
[c] Institute of Atomic and Molecular Physics, Sichuan University, Chengdu 610065, China
[d] Shanghai Institute of Applied Physics, Chinese Academy of Sciences, Shanghai 201203, China

HIGHLIGHTS

- High pressure behaviors of TiO_2 and TiO_2(B) coexisting nanosheets were investigated.
- The anatase phase existed and TiO_2(B) phase almost cannot be observed upon compression.
- The unique high pressure behaviors were discussed.
- The coexistence nanosheet has high incompressibility.

ARTICLE INFO

Article history:
Received 10 October 2015
Accepted 10 November 2015
Available online 14 November 2015

Keywords:
Nanosheets
High pressure
Phase transition
Synchrotron radiation
Raman spectroscopy

ABSTRACT

High pressure behaviors of anatase TiO_2 and TiO_2(B) coexisting nanosheets were investigated using *in situ* synchrotron X-ray diffraction and Raman Spectroscopy. The X-ray diffraction revealed that upon compression an α-PbO_2 phase appeared at 11.4 GPa, and then the baddeleyite phase appeared at 23.6 GPa. Upon decompression the anatase phase still existed obviously and TiO_2(B) phase almost cannot be observed. The Raman spectrum at ambient pressure presented the typical curve of anatase TiO_2, however the pressure dependence for compression and decompression did not show the common phase transion from anatase to α-PbO_2 or to baddeleyite. This is different from high pressure behaviors of other TiO_2 nanostructures and could be attributed to the existence of small amount of TiO_2(B) at the starting materials. The pressure relationship of the Raman frequencies shift slope indicated the coexistence nanosheet has high incompressibility compared with other TiO_2 nanomaterials and corresponding bulks.

1. Introduction

Titanium dioxide (TiO_2) nanomaterials have been intensively investigated because of its superior physical and chemical properties, which have been widely applied in photocatalysis (Chenbiao et al., 2013), dye-sensitized solar cells (DSCs) (O'Regan and Grätzel, 1991), energy conversion and storage devices (Xujie et al., 2014; Shen et al., 2011), gas sensors (Al-Homoudi et al., 2007), transparent conductive oxide (TCO) films (Hitosugi et al., 2010), etc. High pressure is one of the state parameters which can provide a clean way to tune interatomic distances and hence formation of new structural properties. In recent years, high-pressure technique began to be employed to study the stabilities and the structural transitions of TiO_2 nanomaterials for exploring the potential application in material science and geosciences (Nishi et al., 2014). Some literatures have reported the high pressure behaviors of TiO_2 nanomaterials intensively depend on both the sizes and the morphologies of starting materials. For instance, a unique size-dependent phase transition selectivity under high pressure exist in nanocrystalline anatase TiO_2: Crystallites with sizes >50 nm transform to orthorhombic α-PbO_2 and then to monoclinic baddeleyite phase; 12–50 nm particles transform to baddeleyite-structure; smaller nanocrystals <10 nm appeared to be amorphous (Swamy et al., 2005; Varghese et al., 2006; Swamy et al., 2009; Wang et al., 2008).

Morphology-dependent phase transitions of anatase TiO_2 presented different phase processes. Morphology-tuned and high pressure driven phase transition of TiO_2 have been observed in

* Corresponding authors.
E-mail addresses: yanwei.huang@hpstar.ac.cn (Y. Huang), wanglin@hpstar.ac.cn (L. Wang).

http://dx.doi.org/10.1016/j.radphyschem.2015.11.008
0969-806X/

nanowires, nanoporous, nanorods, nanobelts, and so on (Quanjun et al., 2013). A direct anatase-to-baddeleyite transformation at ~9 GPa for nanowires was found, which was clearly different from the size-dependent phase transition behaviors for nanocrystalline TiO_2, besides the higher compressibility in the *c*-axis compared to the a-axis. The nanoporous structure first starts to transform into the baddeleyite phase with poor crystallinity at ~15.2 GPa which coexists with anatase phase up to 18.4 GPa, and then transform into an amorphous phase above 20.5 GPa. This phenomenon is different from the pressure-induced amorphization of the nanoparticles. These results indicate that nanomaterials with different sizes and morphologies go through unique phase transition process and sequences due to their finite-size limit effect and special nanostructures.

TiO_2 has four main polymorphs anatase, rutile, brookite, and TiO_2(B), among them, the anatase phase TiO_2 has received numerous research because of its typical crystal structure and noticeable size effects. TiO_2(B) is rarely available in nature, and the phase structure is less compact than that of other forms of TiO_2. The volume of a TiO_2 unit in TiO_2(B) is 35.27 $Å^3$ as compared with 31.12 $Å^3$ for rutile, 32.20 $Å^3$ for brookite and 34.02 $Å^3$ for anatase phases (René et al., 1980). TiO_2(B) has a monoclinic C2/m structure comprised of edge- and corner-sharing TiO_6 octahedra with an open channel parallel to the *b*-axis sitting between axial oxygens. The TiO_2(B) polymorph is in focus of recent studies regarding its usage as high power and high capacity anode materials because of its stability over multiple lithiation/delithiation cycles which has the potential applications for electric vehicles and grid storage (Dylla et al., 2013).

In this paper, we studied the pressure-induced structural phase transitions in coexisting anatase and TiO_2(B) phases in form of nanosheets using *in situ* synchrotron X-ray diffraction (XRD) and Raman spectroscopy in diamond anvil cells (DACs) at room temperature. The XRD result supported the partial phase transition from anatase to α-PbO_2 and then to baddeleyite phase, which is similar with reported properties of TiO_2 nanostructure under high pressure. However, the pressure dependence of Raman spectra during compression and decompression processes did not clearly show the common phase transion from anatase to α-PbO_2 or to baddeleyite. Meanwhile, the pressure relationship of the Raman frequencies shift slope indicated the coexisting nanosheet has high incompressibility compared with other TiO_2 nanomaterials and corresponding bulks. This is different from high pressure behaviors of other TiO_2 nanostructures and could be ascribed to the existence of small amount of TiO_2(B) at the starting materials.

2. Experimental details

The TiO_2 nanosheets were synthesized by a simple hydrothermal route using 25 ml Titanium butoxide, $Ti(OC_4H_9)_4$, and 4 ml hydrofluoric acid solution (concentration 40%) as precursors which is similar to the description in the previous reports (Zhang et al., 2012). In the concrete process, the $Ti(OC_4H_9)_4$ and HF were mixed in a Teflon-lined autoclave with a capacity of 100 ml then kept at 180 °C for 24 h. The precipitates were then separated from the suspension by centrifugation (4000 rpm, 15 min). The products were further suspended and centrifuged in absolute ethanol three times, followed by drying under an infrared lamp. High pressure XRD experiments were performed at the 15U1 beamline of Shanghai Synchrotron Radiation Facility (SSRF). The incident wavelength of the beam is 0.6199 Å with a beam size of 2×7 μm^2. The high pressure measurements were carried out at room temperature by using a gasketed high pressure DAC. To produce a qusi-hydrostatic environment around sample, we used a 4:1 mixture of methanol:ethanol as a pressure transmitting medium. Pressure was determined by pressure dependent spectral shift of the sharp ruby fluorescence R1 line (Mao et al., 1978; Wang and Saxena, 2001) The sample was placed in a stainless steel gasket hole 150 μm in diameter with the diamond culet size of 500 μm in diameter. High pressure Raman scattering measurements were performed using a Renishaw inVia Raman spectrometer with excitation wavelength of 633 nm. Morphologies of the sample was characterized by field emission scanning electron microscope (SEM) (S-4800, Hitachi, Japan) at accelerating voltage of 20 kV.

3. Results and discussion

Anatase TiO_2 and TiO_2(B) phase structure are built up with tetragonal $I4_1/amd$ structure and monoclinic C2/m structure, respectively, as shown in Fig. 1. Both of the unit cells contain TiO_6

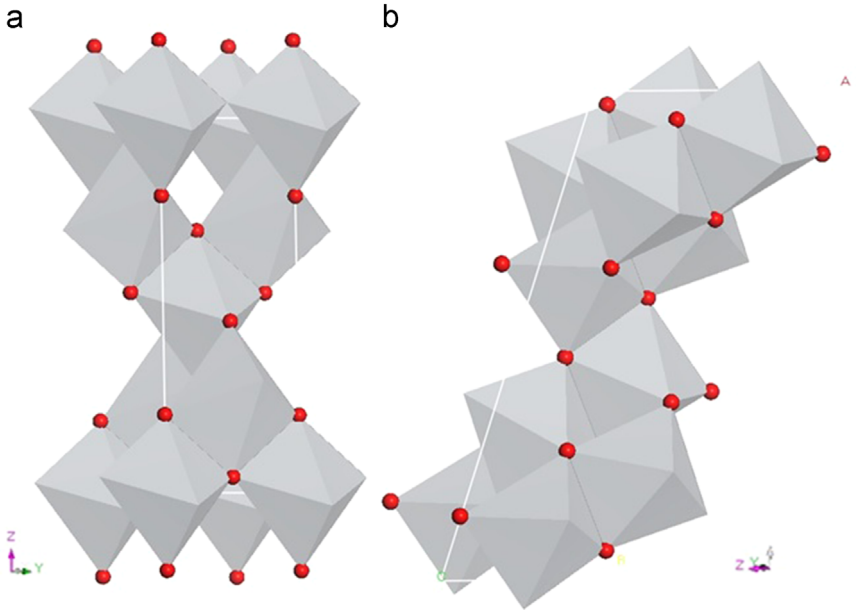

Fig. 1. The polyhedron structures of anatase TiO_2 (a) and TiO_2(B) phase (b).

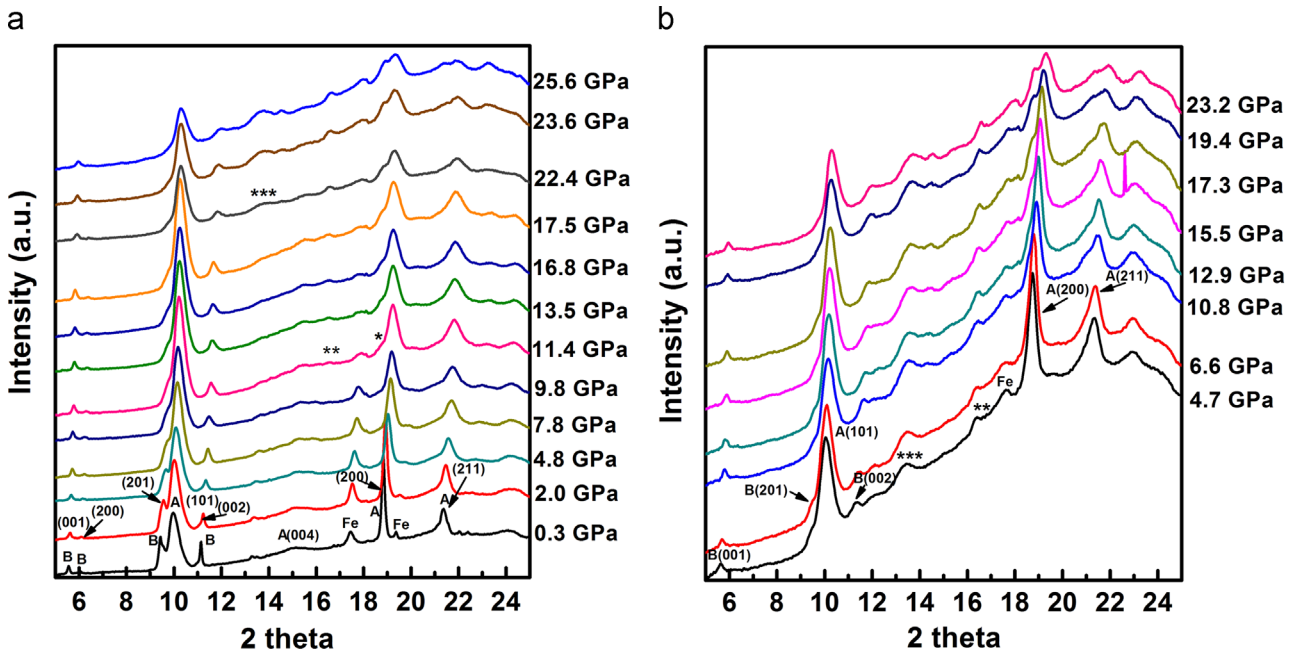

Fig. 2. Synchrotron XRD patterns of TiO_2 nanosheets under high pressure. (a) Compression; (b) Decompression.

octahedra, but the linkage between the octahedra is different. The anatase structure has edge-shared TiO_6 octahedra and TiO_2(B) structure is comprised of edge- and corner-shared TiO_6 octahedra. In fact, TiO_2(B) could be seen as distorted octahedra structure. It is relatively difficult to synthesize pure anatase or TiO_2(B) phase, and the two-phase coexisting phenomenon is very common. Here we study the stability and phase transition of co-existing nanosheets of anatase/TiO_2(B) and try to figure out the pressure-dependent relationship.

Fig. 2 shows the pressure evolution of synchrotron XRD patterns for TiO_2 nanosheets with compression (a) and decompression (b) processes. The diffraction peaks identified in starting structure were found to be consistent with the diffraction planes of tetragonal antase TiO_2 (marked with A) and monoclinic TiO_2(B) (marked with B), agreeing with the standard JCPDS file No. 21-1272 and No. 46-1238, respectively. Two peaks of iron marked as Fe. As shown in Fig. 2(a), during compression, an α-PbO_2 phase appeared when the pressure reached 11.4 GPa, while the peaks in anatase phase are gradually broadened and weakened which indicate that the anatase phase starts to transform into α-PbO_2 phase (marked with * and **). For the TiO_2(B) phase, the peak (201) gradually becomes weakened with increasing pressure and disappeared at 11.4 GPa, at the same pressure where α-PbO_2 phase appeared. Above 13.5 GPa, the α-PbO_2 phase appeared clearly and the diffraction peaks for antase phase continue to be broadened and weakened. At 22.4 GPa, the baddeleyite phase appeared, marked with *** as shown in Fig. 2(a), and with further increase of pressure, the baddeleyite peak become more clear. However, until the maxium pressure of 25.6 GPa the common pressure-induced amorphization effect in TiO_2 nanoparticles cannot be observed for this system. Upon the decompression as shown in the Fig. 2(b), the anatase phase almost maintained initial state, and TiO_2(B) phase has been almost removed when the pressure was released to 4.7 GPa. Moreover, the α-PbO_2 phase (marked with *), agreeing with the (211) plane in α-PbO_2-type TiO_2 (Meng et al., 2008), disappeared during the decompression process. This means this plane in α-PbO_2 phase can be reversibly decompressed. The anatase phase is always existing for both compression and decompression process. This result is a little different from previous reports (Li et al., 2014), where the anatase phase transforms into the baddeleyite structure completely at 20–23 GPa. According to the aforementioned three phase transition regimes existing in anatase TiO_2 nanoparticles: phase transition from anatase to α-PbO_2 and then to baddeleyite phase in >50 nm, we speculate it should be ascribed to the size of nanosheet. From the image of scanning electron microscope (SEM), it can be seen that the thickness of nanosheets should be almost 50–100 nm shown in Fig. 3. We think this may be attributed to the existence of TiO_2(B) phase in the starting anatase structure, and it is interesting that coexistence might postpone or elevate the pressure of amorphization. In addition, it is worth noting that TiO_2(B) phase presents a trend to be weakened with increasing of pressure and almost fading away in the process of decompression. This maybe provide a new method for removing undesirable phase and obtaining certain pure sample by applying high-pressure.

The pressure dependence of the d-spacings is illustrated in Fig. 4, in which A(101) corresponds to the peak (101) for anatase and B(001) denotes the peak (001) for TiO_2(B) phase. We observed the d-spacings decrease with increasing pressures. During the compression, the peak B(200) and B(201) continue up to the pressure of 9.8 GPa and almost disappeared. It can be detected when the exposure time is prolonged, but the d-spacings still have the trend of reduction with increasing pressure. However, during the decompression, the peak B(200) and B(201) did not appear again which indicated the irreversible phase transition of TiO_2(B). The d-spacings of the planes of A(200) and A(211) are decreasing during the compression until 25.6 GPa and increased very little when the pressure was released. This indicate the beared stability of anatase TiO_2 phase on the whole process of compression and decompression. The peak marked with Fe vanished with increasing pressure because the sample chamber by stainless steel gasket is enlarging.

Fig. 5 shows the evolution of the volume with pressure changing. The pressure–volume data of anatase phase and TiO_2(B) phase were fitted to the third-order Birch–Murnaghan equation of state. The bulk modulus (B_0) of the anatase and TiO_2(B) phase were determined to be 125 GPa and 321 GPa, respectively, with the second derivative (B_0') being fixed at 4. In the coexisting phase, the bulk modulus of anatase phase is much smaller than those of reported nanoparticles (180–240 GPa) (Li

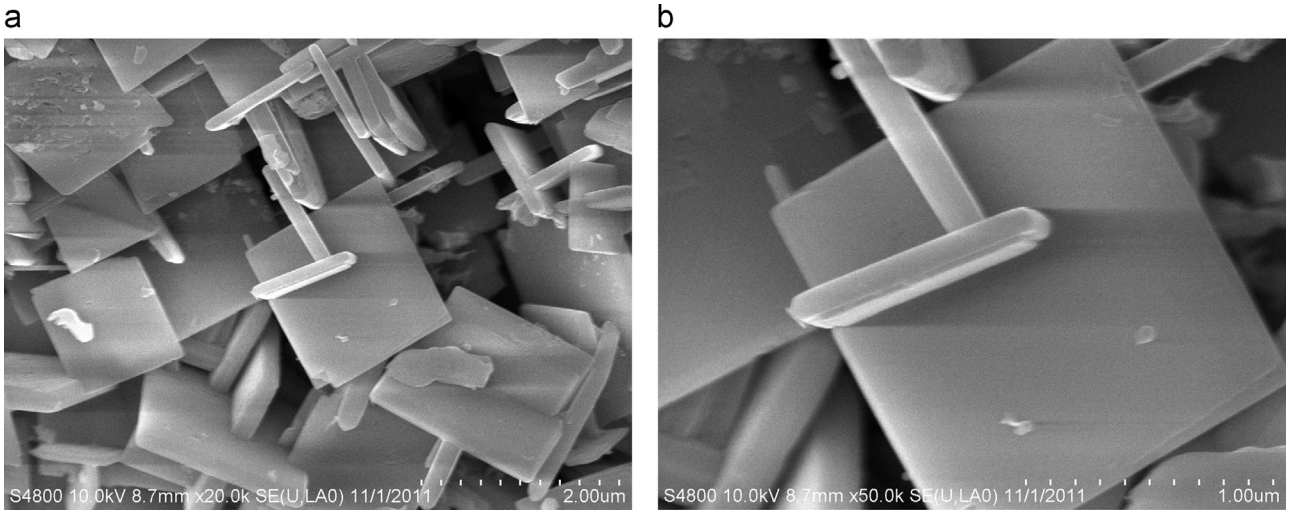

Fig. 3. The SEM images of TiO_2 nanosheets.

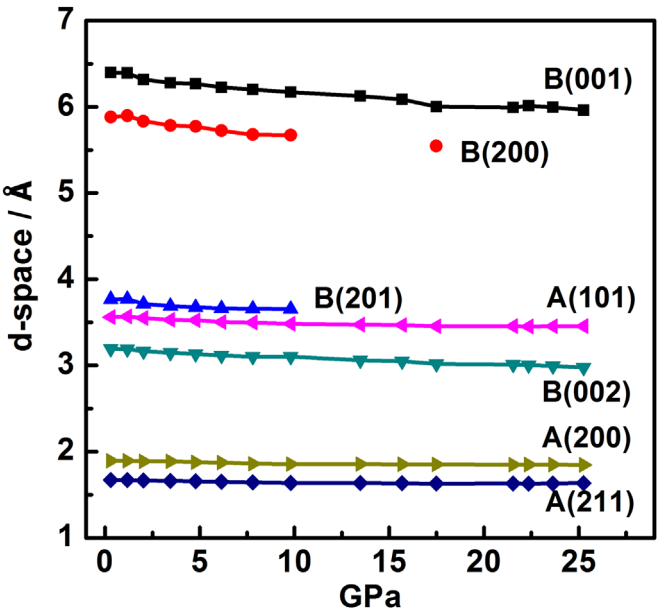

Fig.4. The illustration of pressure dependence of the d-spacings for TiO_2 nanosheet.

et al., 2014), but that of TiO_2(B) is much higher and almost similar to the reported rice-shape nanoparticles (Seung-won et al., 2008) and pure anatase TiO_2 nanosheets (Li et al., 2014).

Fig. 6 shows the Raman spectra of TiO_2 nanosheets during compression (a) and decompression (b). In Fig. 6(a), at ambient pressure, there are almost six Raman active modes observed at 147 cm^{-1}(E_g), 204 cm^{-1}(E_g), 392 cm^{-1}(B_{1g}), 512 cm^{-1}(A_{1g} and B_{1g}), and 635 cm^{-1}(E_g) which agree with the TiO_2 anatase structure according to previous reports (Li et al., 2014). The TiO_2(B) phase has not be detected which could be explained like this: Both TiO_2(B) and anatase structure are comprised of TiO_6 octahedra, but the octahedra in TiO_2(B) structure are a little distorted. Besides, the predominant phase in this nanosheet is anatase not TiO_2(B) which can be seen from the intensity change in synchrotron XRD. With the pressure increasing, the Raman peak 204 cm^{-1}(E_g) disappeared at the 7.2 GPa, and all other Raman bands showed blueshift and became weaker and broader. When the pressure achieved 16.9 GPa, the Raman peak 147 cm^{-1}(E_g) changed and split into two peaks which revealed new phase formed. This should be attributed to appearance of α-PbO_2-type TiO_2, and the new peak accords with (211) plane in α-PbO_2 phase, which has been marked with * in Fig. 2(a). Its intensity is becoming obvious and dominant with rising pressure while upon decompression the intensity of the new peak turns weak shown in

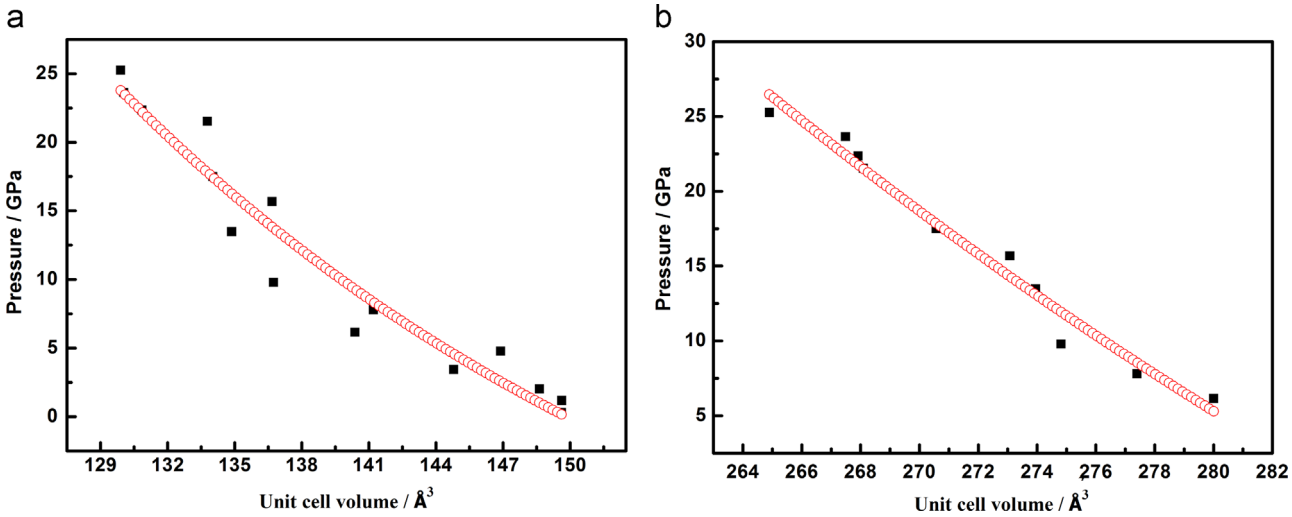

Fig. 5. The pressure–volume diagram of TiO_2 nanosheets for anatase phase (a) and TiO_2(B) phase (b).

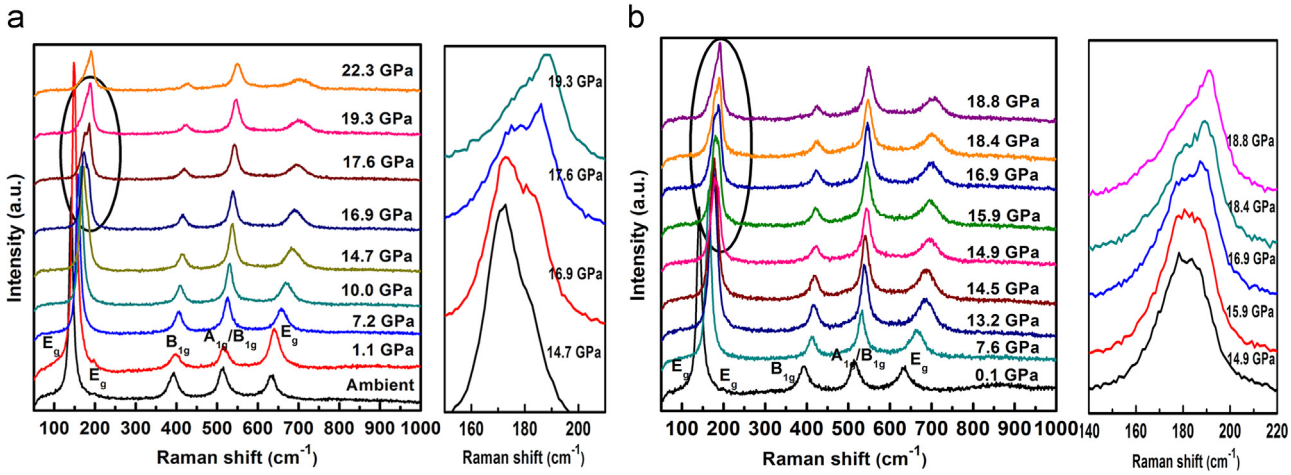

Fig. 6. Raman spectra of the TiO_2 nanosheets at various pressure: (a) compression and (b) decompression. The right image is the enlarging of ellipse in the left graph.

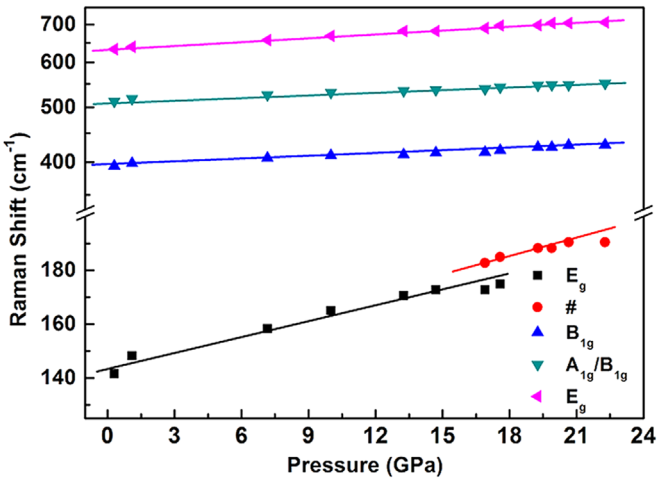

Fig. 7. Pressure dependence of the peak frequencies of Raman spectra for the TiO_2 nanosheets.

Fig. 6(b). When the pressure is released to 15 GPa the Raman peak 147 cm^{-1}(E_g) almost recovered, which revealed the (211) plane in α-PbO_2 phase could be reversible during the whole compression and decompression. It also can be seen from XRD results in Fig. 2. This is very interesting and different from previous studies about TiO_2 nanomaterials and need further investigation. For the reported Raman spectra of nanoporous TiO_2, two weak peaks occurred at 258 cm^{-1} and 497 cm^{-1} ascribed to baddeleyite phase when the pressure reached ~15 GPa, and the anatase phase completely converted into an amorphous form when the pressure was beyond 18 GPa. For the reported Raman spectra of pure anatase TiO_2 nanosheets, an additional Raman band at 490 cm^{-1} happened at 16.7 GPa meaning phase transition. Here, the TiO_2 nanosheets do not become amorphous from the beginning to the end during compression which partially could be due to the larger crystal size. Again, when the pressure is released to ambient pressure, the quenched sample recovered its initial state from the Raman Spectra which conformed to be anatase structure from the results of XRD.

As shown in Fig. 7, all the four strong Raman peaks, assigned to two E_g modes and one B_{1g} mode and one A_{1g}/B_{1g} duplicated mode, shift to higher frequencies under compression. The pressure dependence of the Raman frequencies shift slope have been linearly fitted over the compression. The fitted values correspond to the peaks of E_g (147 cm^{-1}), B_{1g} (392 cm^{-1}), A_{1g}/B_{1g} (512 cm^{-1}), and E_g (635 cm^{-1}) modes are 1.82 cm^{-1}/GPa (0.13), 1.50 cm^{-1}/GPa (0.08), 1.66 cm^{-1}/GPa (0.06), and 3.39 cm^{-1}/GPa (0.09), respectively. The new peak appearing (marked with #) at 16.9 GPa has the pressure coefficient of 1.48 cm^{-1}/GPa (0.25). The average slope of the intense E_g band (located at 147 cm^{-1}) is smaller than that of anatase nanoparticles (2.58 cm^{-1}/GPa), nanoporous anatase TiO_2 (2.84 cm^{-1}/GPa) and bulks (2.7 cm^{-1}/GPa)(Wang and Saxena, 2001; Hearne et al., 2004). This might indicate that the anatase and TiO_2(B) coexisting nanosheet structure has a strong incompressibility compared with other TiO_2 nanostructures and corresponding bulks.

4. Conclusions

The high pressure driven structural transitions were studied by *in situ* synchrotron radiation and Raman spectroscopy in anatase TiO_2 and TiO_2(B) coexisting nanosheets as starting material. The XRD results revealed the partial phase transition from anatase to α-PbO_2 and then to baddeleyite phase. The anatase phase was dominating phase and TiO_2(B) phase almost cannot be observed with increasing pressure. The pressure-induced amorphization phenomenon did not happen until the pressure is 25.6 GPa, which is different from amorphization of other TiO_2 nanoparticles below 20 GPa, When the pressure was released to ambient pressure, the anatase phase dominate the structure without the TiO_2(B) phase. From the pressure dependence in Raman spectrum the common phase transion from anatase to α-PbO_2 or to baddeleyite could not almost be detected and the nanosheet showed incompressibility compared with other reported TiO_2 nanomaterials and corresponding bulks.

Acknowledgments

We acknowledge the support of NSAF (Grant No. U1530402) and Natural Science Foundation of China (Grant No.10904022 and No. 61504034). The authors are also grateful to Ke Yang (Shanghai Synchrotron Radiation Facility, SSRF) for X-ray diffraction measurements, and J. Zhang (Hangzhou Dianzi University) for the synthesized sample and scanning electron microscopy.

References

Xu, Chenbiao, Yang, Wenshao, Guo, Qing, Dai, Dongxu, Chen, Maodu, Yang, Xueming, 2013. Molecular hydrogen formation from photocatalysis of

methanol on TiO_2 (110). J. Am. Chem. Soc. 135, 10206.
O'Regan, B., Grätzel, M., 1991. A low cost, high-efficiency solar cell based on dye-sensitized colloidal TiO_2 films. Nature 353, 737.
Xujie, L.ü, Wenge, Yang, Zewei, Quan, Tianquan, Lin, Ligang, Bai, Lin, Wang, Fuqiang, Huang, Yusheng, Zhao, 2014. Enhanced electron transport in Nb-doped TiO_2 nanoparticles via pressure-induced phase transitions. J. Am. Chem. Soc. 136, 419–426.
Shen, L., Zhang, X., Li, H., Yuan, C., Cao, G., 2011. Design and tailoring of a three-dimensional TiO_2-graphene–carbon nanotube nanocomposite for fast lithium storage. J. Phys. Chem. Lett. 2, 3096.
Al-Homoudi, Ibrahim A., Thakur, J.S., Naik, R., Auner, G.W., Newaz, G., 2007. Anatase TiO_2 films based CO gas sensor: film thickness, substrate and temperature effects. Appl. Surf. Sci. 253, 8607–8614.
Hitosugi, Taro, Yamada, Naoomi, Nakao, Shoichiro, Hirose, Yasushi, Hasegawa, Tetsuya, 2010. Properties of TiO_2-based transparent conducting oxides. Phys. Status Solidi A 207, 1529–1537.
Nishi, M., Irifune, T., Tsuchiya, J., Tange, Y., Nishihara, Y., Fujino, K., Higo, Y., 2014. Stability of hydrous silicate at high pressures and water transport to the deep lower mantle. Nat. Geosci. 7, 224–227.
Swamy, V., Kuznetsov, A., Dubrovinsky, L.S., 2005. Finite-size and pressure effects on the Raman spectrum of nanocrystalline anatase TiO_2. Phys. Rev. B 71, 184302.
Varghese, Swamy, Alexei, Kuznetsov, Dubrovinsky, Leonid S., et al., 2006. Size-dependent pressure-induced amorphization in nanoscale TiO_2. Phys. Rev. Lett. 96, 135702.
Swamy, V., Kuznetsov, A.Y., Dubrovinsky, L.S., et al., 2009. Unusual compression behavior of anatase TiO_2 nanocrystal. Phys. Rev. Lett. 103, 075505.
Wang, Y.J., Zhao, Y.S., Zhang, J.Z., Xu, H.W., et al., 2008. In situ phase transition study of nano- and coarse-grained TiO_2 under high pressure/ temperature conditions. J. Phys.: Condens. Mater. 20, 125224.
Quanjun, Li, Benyuan, Cheng, Xue, Yang, Ran, Liu, et al., 2013. Morphology-tuned phase transitions of anatase TiO2 nanowires under high pressure. J. Phys. C. hem. C 117, 8516–8521.
René, Marchand, Luc, Brohan, Michel, Tournoux, 1980. A new form of titanium dioxide and the potassium octatitanate $K_2Ti_8O_{17}$. Mater. Res. Bull. 15, 1129–1133.
Dylla, Anthony G., Henkelman, Granme, Stevenson, Keith J., 2013. Lithium insertion in nanostructured TiO_2(B) architectur. Acc. Chem. Res. 46, 1104–1112.
Zhang, Jun, Xi, Junhua, Ji, Zhenguo, 2012. Mo+N codoped TiO_2 sheets with dominant {001} facets for enhancing visible-light photocatalytic activity. J. Mater. Chem. 22, 17700.
Mao, H.K., Bell, P.W., Shaner, J.W., Steinberg, D.J., 1978. Specific volume measurements of Cu, Mo, Pd, and Ag and calibration of the Ruby R1 fluorescence pressure gauge from 0.06 to 1 Mbar. J. Appl. Phys. 49, 3276–3284.
Wang, Zhongwu, Saxena, S.K., 2001. Raman spectroscopic study on pressure-induced amorphization in nanocrystalline anatase(TiO_2). Solid State Commun. 118, 75–78.
Meng, D.W., Wu, X.L., Sun, F., et al., 2008. High-pressure polymorphic transformation of rutile to α-PbO_2-type TiO_2 at {011}R twin boundaries. Micron 39, 280–286.
Li, Quanjun, Cheng, Benyuan, Tian, Baoli, et al., 2014. Pressure-induced phase transitions of TiO_2 nanosheets with high reactive {001} facets. RSC Adv. 4, 12873–12877.
Seung-won, Park, Jung-tak, Jang, Jinwoo, Cheon, et al., 2008. Shape-dependent compressibility of TiO_2 anatase nanoparticles. J. Phys. C.hem. C 112, 9627–9631.
Wang, Zhongwu, Saxena, S.K., 2001. Raman spectroscopic study on pressure-induced amorphization in nanocrystalline anatase (TiO_2). Solid State Commun. 118, 75–78.
Hearne, G.R., Zhao, J., Dawe, A.M., Pischedda, V., Maaza, M., Nieuwoudt, M.K., Kibasomba, P., Nemraoui, O., Comins, J.D., Witcomb, M.J., 2004. Phys. Rev. B 70, 134102.